Oily wastewater treatment using mullite ceramic membrane

Mohsen Abbasi[a], Abdolhamid Salahi[b], Mojtaba Mirfendereski[b], Toraj Mohammadi[c,*], Fatemeh Rekabdar[d], Mahmoud Hemmati[d]

[a]*Department of Applied Chemistry, East Tehran Branch, Islamic Azad University, Tehran, Iran*
[b]*Faculty of Chemical Engineering, Iran University of Science and Technology, Research Centre for Membrane Separation Processes, Narmak, Tehran, Iran*
[c]*Department of Chemical Engineering, South Tehran Branch, Islamic Azad University, P.O. Box 11365-4435, Tehran, Iran*
Tel. +98-21-77240496; Fax: +98-21-77240495; email: torajmohammadi@iust.ac.ir
[d]*Polymer Science and Technology Division, Research Institute of Petroleum Industry (RIPI) Tehran, Iran*

ABSTRACT

This paper presents performance of a microfiltration (MF) ceramic membrane for treatment of oily wastewaters. Mullite MF membranes were synthesized from kaolin clay. The effects of different operating parameters such as pressure (0.5–4 bar), volumetric flow rate (0–2 m/s), temperature (15–55°C), oil concentration (250–3000 ppm) and salt concentration(0–200 g/l) on permeate flux (PF), fouling resistance (FR), fouling and rejection (*R*) were investigated. In order to determine the best operating conditions, 250–3000 ppm condensate gas in water emulsions were employed as synthetic feed. The rejection of total organic carbon (TOC) for the synthetic feeds was found to be more than 94%. The results show that by increasing temperature and pressure, the PF increases. Also, by increasing oil content and salt concentration, the membrane is fouled rapidly and the PF decreases. At low salt concentration (0–25 g/l), PF increases with increasing salt concentration, but at high salt concentration (25–200 g/l), it decreases with increasing salt concentration. Increasing volumetric flow rate causes PF to increase and FR reduce.

Keywords: Ceramic membrane; Oil in water emulsions; Fouling; Rejection; Wastewater treatment; Microfiltration

1. Introduction

A large volume of wastewater in the form of either oil-in-water (o/w) or water-in-oil (w/o) emulsions is generated from various process industries such as metallurgical, transportation, food processing and petrochemical as well as petroleum refineries. Typical composition ranges of 'Produced water' generated in the oily wastewater oil and gas industrial processes include 50–1000 mg/l of total oil and grease and 50–350 mg/l of total suspended solids (TSS). Environmental regulations require that maximum total oil and grease concentration in discharge waters to be 10–15 mg/l [1–3]. Major pollutant in wastewater (also known as produced water) generating from oil field is oil which may range between 100 and 1000 mg/l or more depending on demulsification efficiency and crude oil nature. Removing oil from oil-in-water (oily water) is an important aspect of pollution control. In recent years, stringent legislation has been implemented regarding the discharge consent of oily wastewater. In wastewater treatment plants, many traditional techniques are used for separation of oily wastewater. Free oil can be easily separated by mechanical means such as gravity settling (API separator),

*Corresponding author.

skimming, dissolved airotation, coalescence and centrifuging. For unstable or primary emulsions which contain oil droplets of diameter greater than 100 μm, chemical separation techniques such as occulation and coagulation are applied. But the above techniques have limitations for separation of secondary emulsions which contain oil droplets of diameter less than 20 μm. Membrane separation, developed in the last 50 years, is one of the alternative techniques for separating secondary emulsions [4]. Membrane filtration is playing a very prominent role in treatment of oily wastewaters due to its advantages: no chemical additives are needed to break the emulsions, high chemical oxygen demand (COD) removal efficiencies are achieved and treatment facilities are quite compact and fully automated [5]. Many studies have been done on oily wastewater treatment with different membranes [6–12].

Most of the reported investigations mainly have focused on treating oily waste waters having oil concentration equal to or higher than 1000 ppm. Treatment of oil-in-water emulsions using hydrophilic membranes has more often been reported than hydrophobic membranes [13–15]. Since it is generally accepted that hydrophilic materials are less sensitive to adsorption compared to hydrophobic ones; thus this may be considered as a key to reducing FR and enhancing PF [16–17].

Ceramic membranes have been known for years and used in many different applications depending on their numerous advantages: stability at high temperatures and pressure resistance, good chemical stability, high mechanical resistance, long life and good antifouling properties. Nowadays, ceramic membranes can be obtained with high separations coefficient, but at the same time, this fact supposes low permeate fluxes. For each application, it is necessary to look for the adequate combination between selectivity and permeation. In the literature, there are excellent works about of the treatment of oily wastewaters with ceramic membranes. All of them successfully reduce the oil concentration in water. The reported studies mainly focus the filtration of oily waters for industrial applications from refinery processes. Ceramic MF membrane can be made from alumina, mullite, cordierite, silica, spinel, zirconia and other refractory oxides [18–19]. Symmetric ceramic membranes are obtained by various methods such as extrusion and slip-casting of ceramic powders with the addition of binders. In order to decreases size of holes in surface of membranes for better separation, asymmetric ceramic membranes prepared by sintering or by sol-gel processes. Therefore these membranes become very expensive. In these membranes, mullite ceramic membranes have very high chemical and thermal stability and are very cheap because they can be prepared by extruding and calcining kaolin clay. Price of zenooz

mind kaolin is only 1 $/kg. Approximate price of prepared membranes in this research is about 266 $/m². It must be noted that performance and rejection of these membrane is scantiness lower than existing expensive ceramic membranes.

In this research, capabilities of synthetic MF mullite ceramic membranes for treatment of synthetic oil-in-water emulsions were studied. The effect of influencing parameters such as pressure, volumetric flow rate, concentrations of oil and salt and temperature on PF, FR, fouling and R were investigated.

2. Experimental

2.1. Theory

PF, FR, fouling and R are important parameters in design and construction of MF separation units. PF shows the amount of permeate or the product rate. FR and fouling represents the amount of cake/gel layer formed on the membrane surface and the flux decline. To measure MF efficiency for treatment of oil-in-water emulsions, R is also utilized. PF is measured gravimetrically with an electronic balance via weighting the permeate. In MF process, separation performance of a membrane is denoted in terms of % R of TOC or any other feed components which is calculated as follows:

$$R(\%) = \left(1 - C_p/C_f\right) \times 100 \qquad (1)$$

where C_p represents concentration of a particular component in permeate, while C_f is its feed concentration. PF is volume of permeate (V) collected per unit membrane area (A) per unit time (t):

$$PF = \left(V/At\right) \qquad (2)$$

FR is calculated as follows (Mohammadi, 2007):

$$FR(\%) = \left[\left(\frac{\Delta P}{\mu PF_{ww}}\right) - \left(\frac{\Delta P}{\mu PF_{wi}}\right)\right] \bigg/ \left(\frac{\Delta P}{\mu PF_{wi}}\right) \times 100 \qquad (3)$$

where ΔP is pressure gradient, μ is feed viscosity, PF_{wi} is initial water flux and PF_{ww} is final water flux (after fouling).

2.2. Setup

In order to carry out the experiments almost close to an industrial scale, a pilot plant was designed. The pilot was operated in cross flow mode. The membrane surface area in contact with the feed was equal to 110 cm². The MF cell was installed in a system according to Fig. 1 and all the industrial reservations were considered during the experiments.
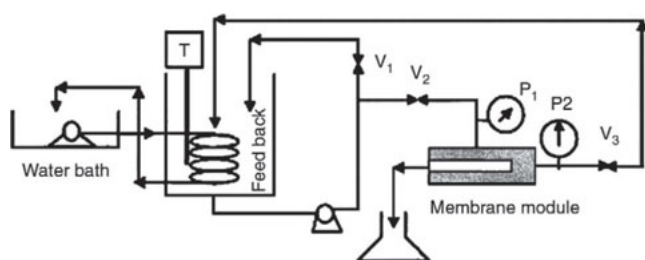
Fig. 1. Microfiltration setup.

The system was simple and had no complexity, however, it was designed in such a way that all important operating parameters in the MF process such as temperature, operating pressure and linear flow velocity could be tuned and controlled. The system mentioned above had a vessel with a capacity of 10 l. This vessel had a heater to heat the feed or to keep it at a constant temperature and also a stirrer in order to keep the feed uniform. The feed temperature was controlled by a digital thermometer with an accuracy of ±0.1°C. A tubular heat exchanger was used to control the feed temperature. Temperature, pressure and flow rate were tuned and controlled simultaneously.

2.3. Membrane preparation

In this research, mullite MF membranes were syntsised from kaolin clay. The kaolin material used obtained from the Zenooz mine in Marand, Iran. The chemical analysis of kaolin is listed in Table 1. Cylindrical shaped (tubular) membranes (i.d.: 9 mm, o.d.:14 mm and l:30 cm) were conveniently made by extruding a mixture of about 62–69% kaolin clay and 38–31% distilled water using an extruder. The cylindrical shaped membrane were then dried at room temperature within 48 h and temperature programmed calcinated at 1250°C for 3 h, suitable calcination period and temperature at which the clay converts to mullite and free silica.

The mullitization reaction takes place when kaolin clay is utilized as the sole source of silica and alumina. The reaction can be represented by the following equation

where the approximate chemical formula for kaolin (without the water of hydration) is given as $Al_2O_3 \cdot 2SiO_2$ and the formula for mullite is given as $3Al_2O_3 \cdot 2SiO_2$:

$$3\left(Al_2O_3 \cdot 2SiO_2\right) \rightarrow 3Al_2O_3 \cdot 2SiO_2 + 4SiO_2 \qquad (4)$$

The term represented by 4 SiO_2 is the free silica generated as a result of the conversion. This free silica was leached and then porous mullite bodies were prepared. Mullite has several distinct advantages over other bodies such as alumina. Since these bodies are heated to high temperatures to achieve the mullite conversion reaction, strong inter-crystalline bonds between mullite crystals, are formed and this results in excellent strength and attrition. Leaching time depends on several factors including the quantity of free silica to be removed, the porosity of the body prior to leaching, concentration of the leaching solution and temperature [20].

Free silica was removed from the calcined membrane by leaching with strong alkali solutions. Removal of this free silica causes microporous tubular ceramic membrane to be made with very high porosity. Free silica removal was carried out with aqueous solutions containing 20% by weight NaOH at a temperature of 80°C for 5 h. Membranes were washed with distilled water for 12 h at a temperature of 80°C in order to remove NaOH. Porosity of the membrane before leaching by water absorption method is 32% while after treatment it increases to 41%. PF of the membrane before and after free silica removal at Pressure (1 bar), Temperature (25°C) and flow rate (1 m/s) for distilled water are 18 and 35 (lit/m² · h), respectively. Fig. 2 shows the surface and cross section of the synthetic mullite ceramic membrane. SEM analysis confirmed that the maximum pore diameter of synthesis membranes is 5 μm. The surface charge of ceramic membrane is anionic and that contact angle is 16°. Characterization of membranes with mercury porosemetery method shows that Total cumulative volume is 0.063 (cc/g), Total specific surface area is 10.27 (m²/g) and Average pore radius of membranes is

Table 1
Analysis of kaolin clay

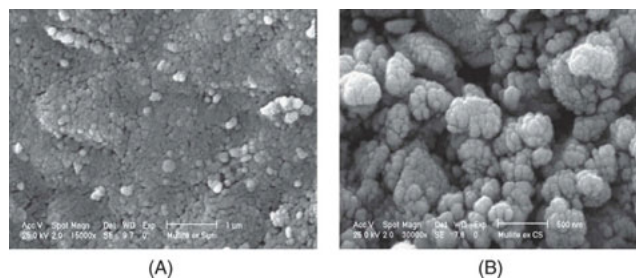| Component	Percent	Phases	Percent
SiO_2	61.62	Kaolinite	64
TiO_2	0.4		
Al_2O_3	24–25	Illite	2.4
Fe_2O_3	0.45–0.65		
K_2O	0.4	Quartz	27
Na_2O	0.5		
LOI	9.5–10	Feldspar	6.6
Total	100		100

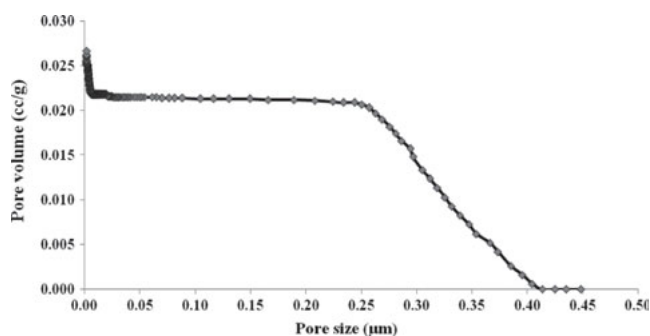Fig. 2. SEM micrographs of the mullite membrane: (A: surface 15000 X) and (B: cross-section 30000 X).

Fig. 3. Pore size distribution of mullite ceramic membranes measured by mercury prosimetery method.

0.289 μm. In addition, Fig. 3 shows particle size distribution of mullite membranes.

2.4. Feed

Oil in water emulsions (oily waters) were prepared by various mixing of condensate gas (C_8–C_{12}) and distillated water with an addition of approximately 0.01wt.% Triton X-100 emulsifier to the mixture for stabilized emulsion. Condensate gas from Seraje Ghom, Iran was used for the preparation of the oil-water emulsions. A blender mixed the oil and water at high shear rates (6000 rpm) for 30 min. Under these conditions, emulsions have a high stability for employing in microfiltration experiments. Particle size distribution of oil droplets in 1000 ppm oil-in-water emulsions has been shown in Fig. 4. Under these conditions, emulsions have high stability for employing in the MF experiments because after 12 h of mixing, don't separate in two phase.

2.5. Analysis of samples

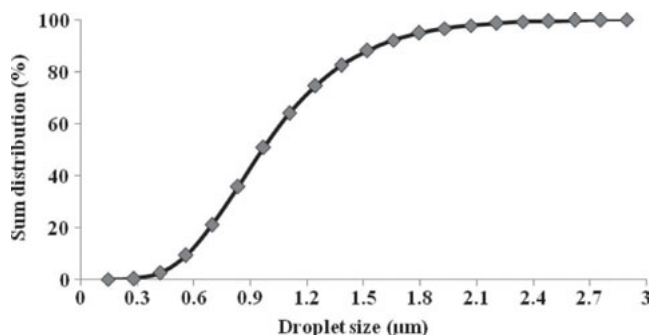Scanning Electron Microscopy (SEM) used in this work was Philips model XL30. Samples for measure-

Fig. 4. Particle size distribution of oil droplets in oil in water emulsion with 1000 ppm oil concentration.

ments of the feed and the permeate total suspended solids (TSS), chemical oxygen demand (COD), turbidity and total organic carbon (TOC) were taken as needed and analyzed by the procedure outlined in standard methods. TOC and Turbidity were estimated using TOC Analyzer (Model DC-190) and Turbidimeter (Model 2100A HACH), respectively.

3. Results and discussions

3.1. Effects of operation conditions on performance of the MF membranes

3.1.1. Effect of pressure

According to the Darcy's law, increasing pressure increases PF, however, fouling restricts this fundamental law. Increasing pressure makes the oil droplets more compact on the membrane surface and blocks the membrane pores [21–24]. Thus, at an best pressure, PF is high, while tendency to cake/gel layer formation is low [21,24]. Effects of pressure on PF, FR and *R* are presented in Figs. 5(a) and 5(b). It can be observed that, with increasing pressure up to 2 bar, PF increases linearly, however, at higher pressure it is nearly constant. This can be due to compression of the cake/gel layer formed on the membrane surface at high pressure. As shown in Fig. 5(a), until a pressure of 2 bar, FR increases slightly with pressure. This can also be due to low tendency to cake/gel layer formation at lower pressure up to 2 bar, and as a result, the FR growth rate is low, however, after that at higher pressure FR more significantly with pressure because the cake/gel layer on the membrane becomes denser.

Fig. 5(b) presents effect of pressure on TOC *R*. The results indicated that *R* increases slightly with increasing pressure. This can also be due to formation of the thicker cake/gel layer, where this layer traps oil droplets among sediment pores and does not let them pass through the membrane.

To achieve an best design, obtaining the maximum PF and considering the minimum investments and operating costs are needed and this means that it is very important to have a membrane with the most effective service time. Primarily, the membrane service time and its PF are affected by concentration polarization (caused by accumulation of solutes) and fouling (formation of a sticky cake/gel layer and/or an irreversible cake/gel layer).

Thus, a pressure of 3 bar can be considered as the best operating pressure. Because at higher pressure, cake/gel layer becomes denser, while PF and *R* does not change any more. In order to observe the effect of pressure on PF as a function of time, some experiments were carried out at a cross flow velocity (CFV) of 1 m/s and temperature of 25°C as presented in Fig. 5(c). In general,

the results illustrated that increasing pressure leads to higher PF values according to According to Darcy's Law. However, at higher pressures, the cake/gel layer formed on the membrane surface is more compressed. This accelerates the membrane fouling [21,24–26]). Thus, at best the pressure, PF is high and tendency to the cake/gel layer formation is low.
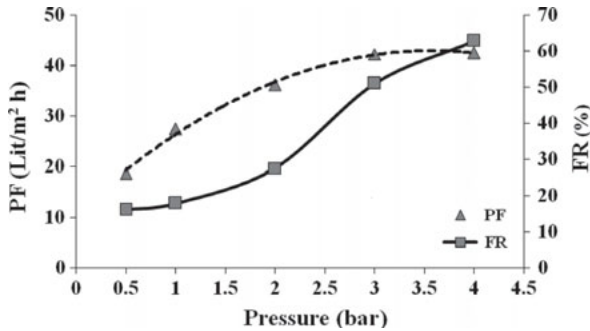
3.1.2. Effect of flow rate

Increasing flow rate increases mass transfer coefficient in the concentration boundary layer and also increases the extent of mixing over the membrane surface. This can reduce aggregation of the feed components in the gel layer, and as a result, the oil droplets on the membrane surface diffuse back to the bulk solution, so the concentration polarization effects diminish. This increases the effective pressure gradient consequently, and thus, PF increases [2,24,27–30]. In Figs. 6(a,b and c), effects of flow rate on PF, FR and R are presented. It can be observed that PF increases with increasing flow rate. The influence of two different flow rates on PF was also compared. At dead end filtration (flow rate equal 0 m/s), there is no turbulency so the cake/gel layer can be formed easily. Therefore, maximum fouling is observed and PF reduced consequently. At low flow rates (0.5 m/s), little turbulency is made so the oil droplets on the membrane surface diffuse back to the bulk solution, and as a result, there is low sediment formation. Thus, PF increase.

Fig. 5(a). Variation of PF and FR with pressure (Flow Rate 1 m/s, oil concentration 1000 ppm, salt concentration 0 ppm and temperature 25°C).

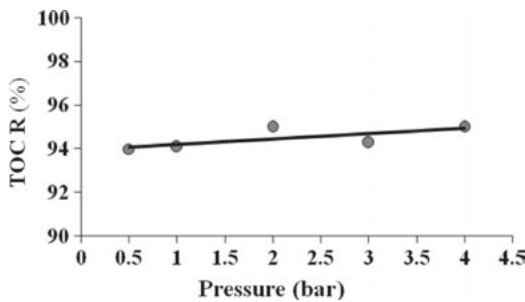
Fig. 5(b). Variation of TOC R with pressure (Flow Rate 1 m/s, oil concentration 1000 ppm, salt concentration 0 g/l, and temperature 25°C).

Fig. 6(a). Variation of PF and FR with flow rate (Pressure 3 bar, oil concentration 1000 ppm, salt concentration 0 ppm and temperature 25°C).
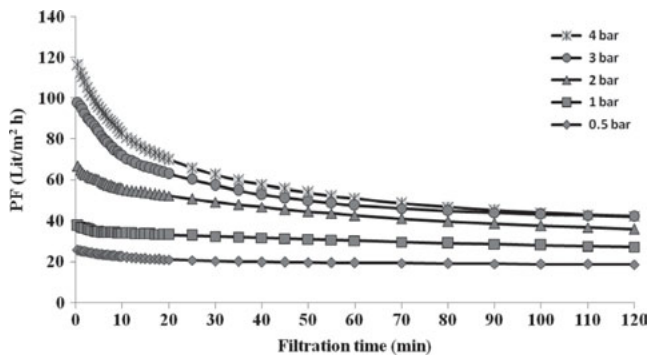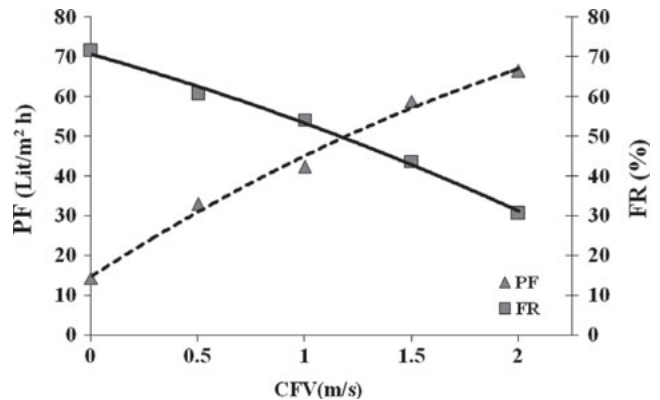

Fig. 5(c). Variation of PF with time as a function of pressure (Flow rate 1 m/s, oil concentration 1000 ppm, salt concentration 0 ppm, and Temperature 25°C).
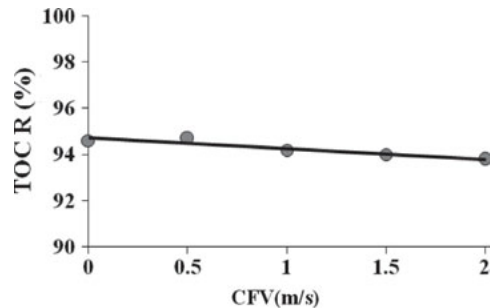

Fig. 6(b). Variation of TOC R with flow rate (Pressure 3 bar, oil concentration 1000 ppm, salt concentration 0 g/l, and temperature 25°C).
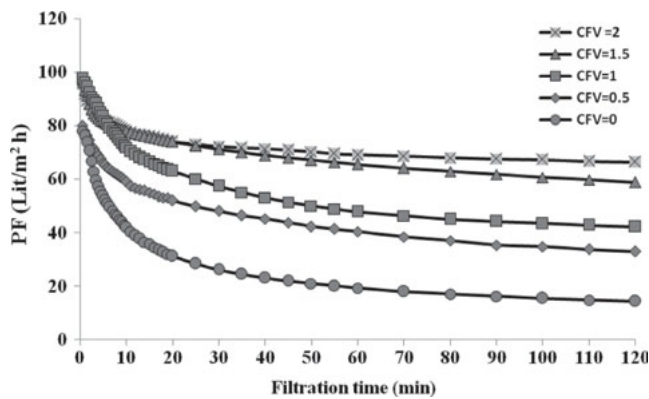
Fig. 6(c). Variation of PF with time as a function of flow rate (Pressure 3 bar, temperature 25°C, oil concentration 1000 ppm and salt concentration 0 ppm).

As shown in Fig. 6(a), increasing flow rate increases Reynolds number and this enhances turbulency, and as a result, PF increases. This is due to reduction of concentration polarization effects. Turbulency on the membrane surface is enhanced by increasing flow rate. Therefore, the oil droplets on the membrane surface return to the bulk solution and concentration polarization effects diminish [24,31,32].

In Fig. 6(b), the effect of flow rate on fractional TOC *R* is shown. According to these results, increasing flow rate causes lower *R*. This is due to removing the oil layer from the membrane surface. This oil layer acts as a dynamic membrane or a barrier against the passage of oil droplets through the membrane.

Variation of PF with time at different flow rates, at a pressure of 3 bar is presented in Fig. 6(c). PF proportionally increases with increasing feed flow rate. Increasing flow rate increases both the mass transfer coefficient in the concentration polarization boundary layer and the degree of mixing near the membrane surface, due to less accumulation of the cake/gel layer on the membrane surface and higher FR. This reduces concentration polarization effects and increases PF [2,24,33]. The same as other results obtained, PF reaches to a constant value after 2 h depending on the flow rate value.

Considering that higher flow rates leads to more power consumption for pumping so the choice of very high flow rates is not economically feasible. Therefore, the best flow rate is 1.5 m/s. By considering cross section of membranes ($A = 6.36 \times 10^{-5}$ m²), 1.5 m/s cross flow velocity is equal to 344 l/h flow rate and for 2 m/s is 467 l/h at condition that pressure is 3 bar. Results from Figs. 6(a and b) show that by increasing flow rate from 344 l/h to 467 l/h at 3 bar pressure, we don't see significant enhancement of PF and also rejection decreases. Therefore it is better to operate process at 1.5 m/s cross flow velocity; else we must use bigger pump with higher energy consumption.

3.1.3. Effect of temperature

As shown in Fig. 7(a), increasing operating temperature increases PF. Also increasing temperature decreases the feed viscosity, and as a result, increases the solvent and the solutes permeabilities (diffusivities) [2,19,32]. As observed in Fig. 7(a), increasing temperature decreases the membrane fouling and this is due to increasing the oil solubility. Thus, PF increases.

According to the results, increasing temperature decreases the *R* (as observed in Fig. 7(b)). This can also be due to the viscosity effect. At higher temperatures, oil and grease can more easily permeate through the membrane.

The results show that the best temperature of 35°C can be recommended to achieve high PF and low FR at low operating costs.

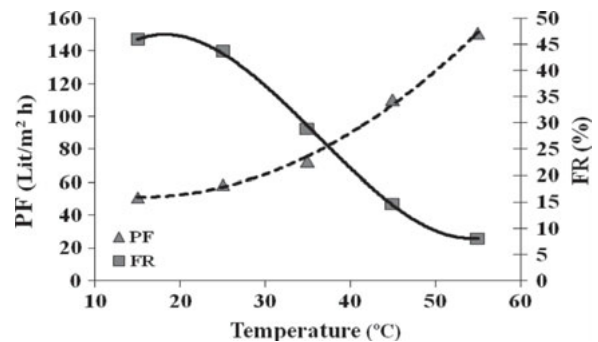Effect of temperature is significant on PF and this can be represented via Arenius equation [22]:

Fig. 7(a). Variation of PF and FR with temperature (Pressure 3 bar, flow rate 1.5 m/s, oil concentration 1000 ppm and salt concentration 0 ppm).
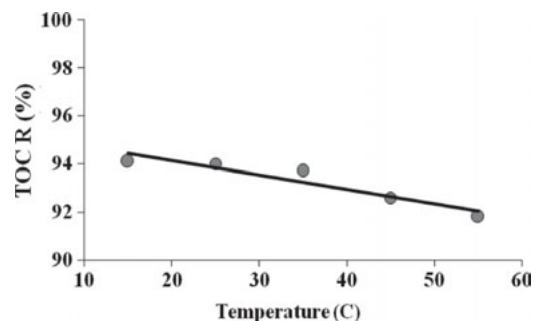

Fig. 7(b). Variation of TOC *R* with temperature (Pressure 3 bar, flow rate 1.5 m/s, oil concentration 1000 ppm and salt concentration 0 g/l).
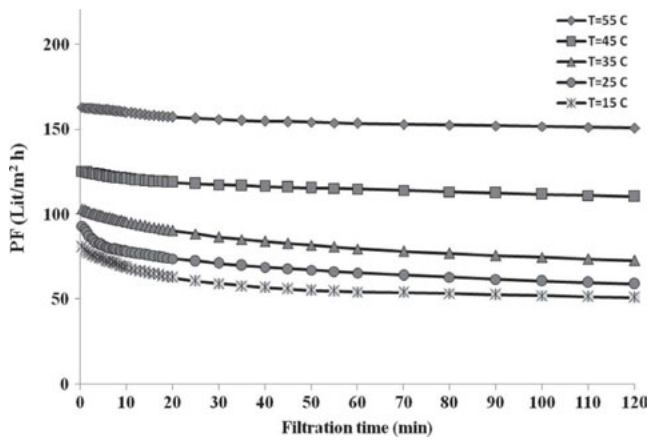
Fig. 7(c). Variation of PF with time as a function of temperature (Pressure 3 bar, flow rate 1.5 m/s, oil concentration 1000 ppm and salt concentration 0 ppm).

$$j = A_P \exp\left(-E_P/RT\right) \tag{5}$$

where A_p is the pre-exponential coefficient and E_p is nominal activation energy of permeation. Also, according to Darcy's Law, increasing temperature increases PF and the experimental data confirm this expectation. It is because viscosity decreases and diffusivity increases at elevated temperatures ([2,24]). Fouling experiments were carried out at different temperatures. The results are shown in Fig. 7(c). As mentioned before, PF reduces with time but generally after 2 h reaches to a constant value depending on the operating temperature. As observed, at higher temperatures, due to lower viscosities and higher difusivities, PF is higher [24].

3.1.4. Effect of oil concentration

Fig. 8(a). shows the effects of oil concentration on PF. Solutions with oil concentrations of 250, 500, 1000, 2000
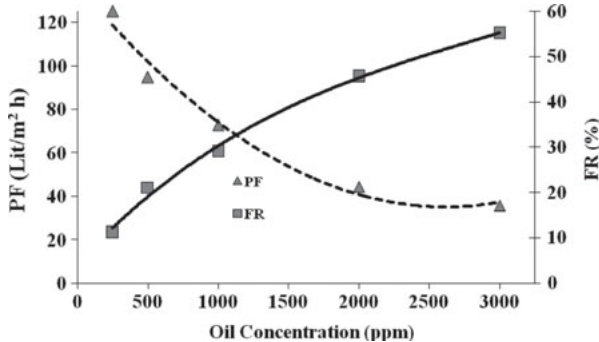

Fig. 8(a). Variation of PF and FR with oil concentration (Pressure 3 bar, flow rate 1.5 m/s, salt concentration 0 ppm and temperature 35°C).
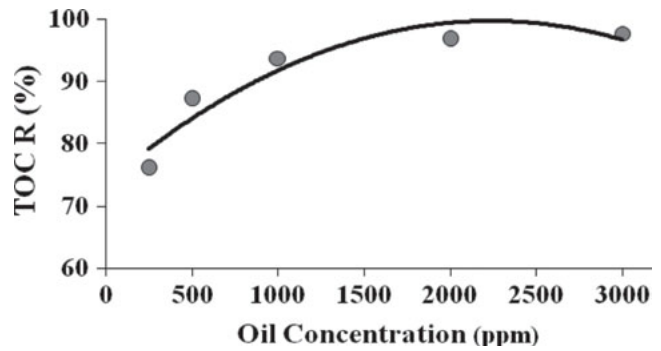

Fig. 8(b). Variation of TOC *R* with oil concentration (Pressure 3 bar, flow rate 1.5 m/s, salt concentration 0 g/l and temperature 35°C).
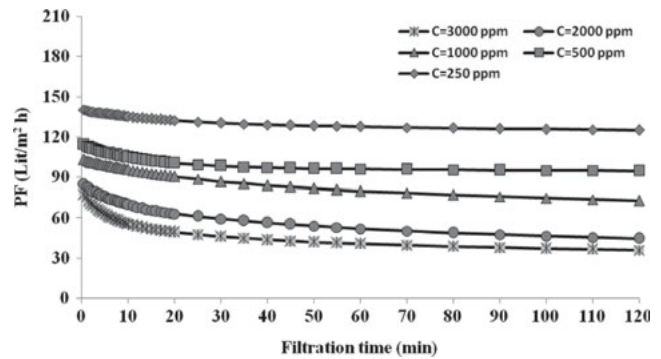

Fig. 8(c). Variation of PF with time as a function of oil concentration (Pressure 3 bar, flow rate 1.5 m/s, salt concentration 0 ppm and temperature 35°C).

and 3000 ppm were prepared. By increasing the concentration from 250 to 3000 ppm, PF decreases because a layer of oil forms on the membrane surface. At lower concentrations, the oil layer formed on the membrane surface can be removed by hydrodynamic action of flow. But at higher concentrations, the hydrodynamic action can not remove the oil layer. By increasing the operation time, this layer becomes thicker and PF decreases [24].

Fig. 8(b) also shows the average TOC *R* at various oil concentrations. The *R* increases from 85.4 to 97.8% with increasing the oil concentration steadily from 250 to 3000 ppm.

Fouling experiments were carried out at different concentrations and the results are shown in Fig. 8(c). As shown, PF decreases quickly at the beginning of the filtration for all concentrations. Also, the PF decline is more severe at higher concentrations. This is because of higher growth rates and thicker layers at higher concentrations.

3.1.5. Effect of salt concentration

Fig. 9(a) shows variations of PF at various salt (NaCl) concentrations (25–200 g/l). As shown, by addition of the salt up to 25 g/l, PF increases and FR decreases but increasing the salt concentration from 25 to 200 g/l causes PF decrease and FR to increase. There are still many debates on the effect of salt concentration on PF [8,33–35]. It can be said that at low salt concentration (25 g/l), high ionic concentration tends to diminish thickness of the double layer around the emulsion droplets, thereby reducing the electrostatic barrier to coalescence, causing high PF and low FR [33]. While at higher salt concentration (50–200 g/l), the viscosity of emulsion increases and the salt crystals foul the membrane pores because of concentration polarization of the salt on the membrane surface, so PF decreases and FR increases (As seen in Fig. 9(b)).

The effect of salt concentration on the TOC R is shown in Fig. 9(c). The results show that the average TOC R is almost the same at different salt concentrations. In fact, the average TOC R is changes from 94.0 to 95.5% when the salt concentrations increase from 25 to
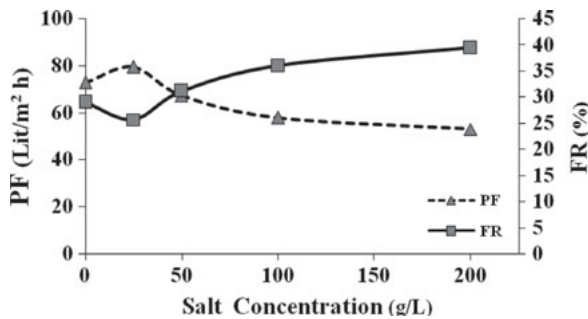

Fig. 9(a). Variation of PF and FR with salt concentration (Pressure 3 bar, flow rate 1.5 m/s, oil concentration 1000 ppm and temperature 35°C).
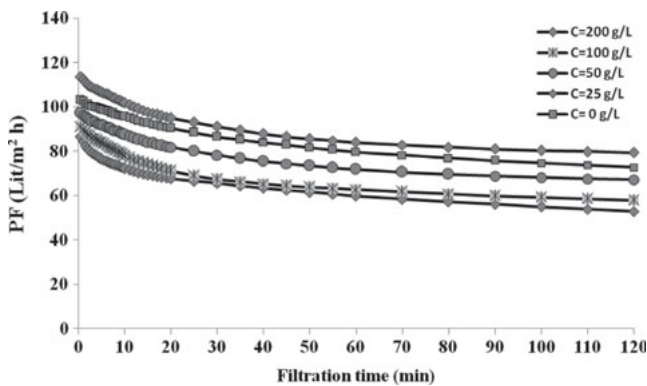

Fig. 9(b). Variation of PF with time as a function of salt concentration (Pressure 3 bar, flow rate 1.5 m/s, oil concentration 1000 ppm and temperature 35°C).
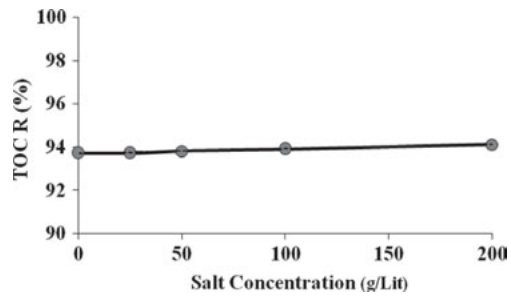

Fig. 9(c). Variation of TOC R with salt concentration (Pressure 3 bar, flow rate 1.5 m/s, oil concentration 1000 ppm and temperature 35°C).

200 g/l. The salt R by the mullite ceramic membrane is very low and is about 5–10%.

3.2. Performance of the MF membranes at best operating conditions

The effect of time on PF at the same operational conditions (best conditions of 3 bar pressure, 1.5 m/s volumetric flow rate, 35°C temperature, 1000 ppm oil-in-water emulsion and 25 g/l salt concentration) is presented in Fig. 10. The results show that PF is nearly constant with time after initial sharp decline. This confirms that the optimal operational conditions were selected correctly. During the first 2 h of filtration, PF steeply decreases. This is followed by a relatively smoother decrease and finally remains almost constant during the last hour of filtration. This can be attributed to the accumulation of droplets oil on the membrane surface and the membrane pores. Table 2 represents characteristics of the MF permeate. From the results presented in Table 2, it can be observed that the treatment efficiency of MF is quite high. This can be attributed to the hydrophilic nature of ceramic membrane material, resulting in a very high effluent quality. Analysis of the permeate revealed very high R for TOC (94.5%) and COD (89%) along with
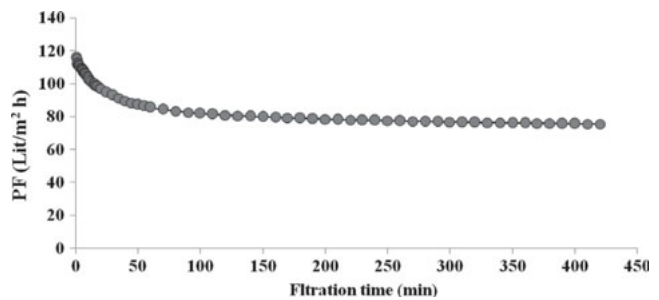

Fig. 10. Variation of PF with time at best operating condition (Pressure 3 bar, flow rate 1.5 m/s, oil concentration 1000 ppm, salt concentration 25 g/l and Temperature 35°C).

Table 2
Characteristics of the wastewater and the treated wastewater

Parameter	Unit	Feed	Permeate
Total suspended solids (TSS)	mg/l	60	Trace
Total dissolve solids (TDS)	g/l	25	23
Chemical oxygen demand (COD)	mg/l	510	54
Total organic carbon (TOC)	mg/l	1000	63
Turbidity	NTU	89	2.3

complete rejection of turbidity and TSS with a reasonably high PF of 75.5 l/(m²h).

Because the mullite ceramic membrane is hydrophilic, the bond between kaolin and the oil layer is very weak and can be broken easily. Therefore, fouling of this membrane is not a major problem, and after 2 h the FR is lower than 30% for a concentration of 1000 ppm. From high chemical and thermal stability of mullite membranes we can select a lot of chemical agent such as NaOH, ethylene diamine tetra acetic acid disodium salt-2-hydrate (EDTA), sodium dodecyl sulfate (SDS) and etc. It must be noted that chemical cleaning mainly involves the dissolution of the material from the membrane surface and several factors could affect chemical cleaning process. These are: temperature, pH, cleaning time and operation conditions such as CFV [32].

4. Conclusion

In this work, treatment of oil-in-water emulsions with synthetic mullite ceramic microfiltration membranes was investigated. According to the obtained results, it can be concluded that MF with mullite ceramic membranes can be used as an advanced method for treatment of the oily waste waters. The results showed that, MF is a feasible and advantageous method for treatment of desalter wastewater effluent. This membrane is very cheap because it can be prepared by extruding and calcining kaolin clay, which comes from the Zenooz mine (Approximate price of prepared membrane is about 266 $/m²) [20]. The results indicated that the ceramic membrane performs high PF and R. The results also indicated that R increases slightly with increasing pressure, salt concentration and oil concentration, also it decrease with increasing volumetric flow rate and temperature. It was observed that PF increases with increasing volumetric flow rate, temperature and pressure, while it decreases with increasing oil concentration. At low salt concentration (0–25 g/l), PF increases with increasing

salt concentration (72.7 to 79.35 l/m²h), but at high salt concentration (25–200 g/l), it decreases with increasing salt concentration (79.35 to 52.93 l/m²h). Increasing volumetric flow rate and temperature causes FR to reduce. The results also showed that the MF treatment is very effective in reduction of TOC (94.5%), TSS and turbidity (about 100%), while it is relatively less effective in reduction of COD (89%) and TDS. The salt R by the mullite ceramic membrane is very low and is about 5–10%. The results showed that a pressure of 3 bar, a flow rate of 1.5 m/s, a temperature of 35°C, an oil concentration of 1000 ppm and a salt concentration of 25 g/l are the best operating conditions. PF of membranes at this condition after 7 h is 75.5 l/(m²h).

Symbols

A	—	Cross section area of membrane (m²)
C	—	Concentration (mg/l)
COD	—	Chemical oxygen demand (mg/l)
CFV	—	Cross-flow velocity (m/s)
d	—	Internal diameter of tubular membrane (m)
FR	—	Fouling resistance
J_W	—	Flux of pure water (l/m²h)
L	—	Tubular membrane length (m)
P	—	Pressure (Pa)
PF	—	Permeate flux (l/m²h)
PF_{wi}	—	Initial water flux (l/m²h)
PF_{ww}	—	Final water flux (after fouling) (l/m²h)
t	—	Time (s)
T	—	Temperature (°C)
TDS	—	Total dissolve solids (mg/l)
TOC	—	Total organic carbon (mg/l)
TSS	—	Total suspended solids (mg/l)
u	—	Cross-flow velocity (m/s)
ΔP	—	Pressure gradient (Pa)
μ	—	Dynamic viscosity (kg/ms)
ρ	—	Density (kg/m³)

References

[1] F.-R. Ahmadun, A. Pendashteh, L.C. Abdullah, D.R.A. Biak, S.S. Madaeni and Z.Z. Abidin, Review of technologies for oil and gas produced water treatment, J. Hazard. Mater., 170 (2009) 530–551.

[2] A. Salahi, T. Mohammadi, A. Rahmat pour and F. Rekabdar, Oily wastewater treatment using ultrafiltration, Desalin. Water Treat., 6 (2009) 289–298.

[3] A. Salahi and T. Mohammadi, Experimental investigation of oily wastewater treatment using combined membrane systems, Water Sci. Technol., 62 (2010) 245–255.

[4] B. Chakrabarty, A.K. Ghoshal and M.K.Purkait, Ultrafiltration of stable oil-in-water emulsion by polysulfone membrane, J. Membr. Sci., (2008) 427–437.

[5] J. Kong and K. Li, Oil removal from oil-in-water emulsions using PVDF membranes, Sep. Purif. Technol., 16 (1999) 83–93.

[6] A. Salahi, M. Abbasi and T. Mohammadi, Permeate flux decline during UF of oily wastewater: Experimental and modeling, Desalination, 251 (2010) 153–160.

[7] L. Yan, S. Hong and M.L. Li, Application of the Al_2O_3-PVDF nanocomposite tublar ultrafiltration (UF) membrane for oily wastewater treatment and its antifouling research, Sep. Purif. Technol., 66 (2009) 347–352.

[8] M. Kuca and D. Szaniawska, Application of microfiltration and ceramic membranes for treatment of salted aqueous effluents from fish processing, Desalination, 241 (2009) 227–235.

[9] R. Ghidossi, D. Veyret and J.L. Scotto, Ferry oily wastewater treatment, Sep. Purif. Technol., 64 (2009) 296–303.

[10] M. Tomaszewska, A. Orecki and K. Karakulski, Treatment of bilge water using a combination of ultrafiltration and reverse osmosis, Desalination, 185 (2005) 203–212.

[11] Y.S. Li, L. Yan and C. Bao, Treatment of oily wastewater by organic–inorganic composite tubular ultrafiltration (UF) membranes, Desalination, 196 (2006) 76–83.

[12] J. Arévalo, G. Garralón, F. Plaza, B. Moreno, J. Pérez and M.A. Gómez, Wastewater reuse after treatment by tertiary ultrafiltration and a membrane bioreactor (MBR): a comparative study, Desalination 243(2009) 32–41.

[13] A. Salahi, A. Gheshlaghi, T. Mohammadi and S.S. Madaeni, Experimental performance evaluation of polymeric membranes for treatment of an industrial oily wastewater, Accepted 9 Jun 2010, Desalination, 262 (2010) 235–242.

[14] M. Abbasi, M.R. Sebzari, A. Salahi, S. Abbasi and T. Mohammadi, Flux decline and membrane fouling in cross-flow microfiltration of oil-in-water emulsions, Desalin. Water Treat., 28 (2011) 1–7.

[15] Y. Zhao, Y. Tan and F.S. Wong, Formation of dynamic membranes for oily water separation by crossflow filtration, Sep. Purif. Technol., 44 (2005) 212–220.

[16] A. Salahi and T. Mohammadi, Oily wastewater treatment by ultrafiltration using Taguchi experimental design, Water Sci. Technol., 63 (2011) 1476–1484.

[17] A. Salahi, R. Badrnezhad, M. Abbasi, T. Mohammadi and F. Rekabdar, Oily wastewater treatment using a hybrid UF/RO system, Desalin. Water Treat., 28 (2011) 75–82.

[18] T. Gallego-Lizon, E. Edwards and G. Lobiundo, Dehydration of water/*t*-butanol mixtures by pervaporation: comparative study of commercially available polymeric, microporous silica and zeolite membranes, J. Membr. Sci., 197(2002) 309–319.

[19] M. Abbasi, M.R. Sebzari and T. Mohammadi, Enhancement of oily wastewater treatment by ceramic microfiltration membrans using powder activated carbon, Chem. Eng. Technol. (2011), DOI: 10.1002/ceat.201100108.

[20] M. Kazemimoghadam, A. Pak and T. Mohammadi, Dehydration of water/1–1dimethylhydrazine mixtures by zeolite membranes, Microporous Mesoporous Mater., 56 (2002) 81–88.

[21] Z. Xiang-hua, Y. Shui-li, W. Beii-fu and Z.Hai-feng, Flux enhancement during ultrafiltration of produced water using turbulence promoter, J. Environ. Sci., 18 (2006) 1077–1081.

[22] T. Mohammadi and A. Esmaeelifar, Wastewater treatment using ultrafiltration at a vegetable oil factory, Desalination, 166 (2004) 329–337.

[23] D. Sun, X. Duan, W. Li and D. Zhou, Demulsification of water-in-oil emulsion by using porous glass membrane, J. Membr. Sci., 146 (1998) 65–72.

[24] T. Mohammadi and A. Esmaeelifar, Wastewater of a vegetable oil factory by a hybrid ultrafiltration-activated carbon process, J. Membr. Sci., 254 (2005) 129–137.

[25] M. Ebrahimi, D. Willershausen, K.S. Ashaghi, L. Engel, L. Placido, P. Mund, P. Bolduan and P. Czermak, Investigations on the use of different ceramic membranes for efficient oilfield produced water treatment, Desalination, 250 (2010) 991–996.

[26] C.B. Spricigo, A. Bolzan and R.A.F. Machado, Separation of nutmeg essential oil and dense CO_2 with a cellulose acetate reverse osmosis membrane, J. Membr. Sci., 188 (2001) 173–179.

[27] K. Scott, A.J. Mahmood, R.J. Jachuck and B. Hu, Intensified membrane filtration with corrugated membranes, J. Membr. Sci., 173 (2000) 1–16.

[28] P. Wang, N. Xu and J. Shi, A pilot study of the treatment of waste rolling emulsion using zirconia microfiltration membranes, J. Membr. Sci., 173 (2000) 159–166.

[29] M.C.V. Vela and S. Blanco, Analysis of membrane pore blocking models applied to the ultrafiltration of PEG, Sep. Purif. Technol., 62 (2008) 489–498.

[30] M. Abbasi, A. Salahi, M. Mirfendereski, T. Mohammadi and A. Pak, Dimensional analysis of permeation flux for microfiltration of oily wastewaters using mullite ceramic membranes, Desalination, 252 (2010) 113–119.

[31] S.S. Madaeni, The effect of large particles on microfiltration of small particales, J. Porous Mater., 18 (2001) 143–148.

[32] T. Mohammadi and M. Kazemimoghadam, Chemical cleaning of ultrafiltration membrane in the milk industry, Desalination, 204 (2007) 213–218.

[33] F.L. Hua, Y.F. Tsang and Y.J. Wang, Performance study of ceramic microfiltration membrane for oily wastewater treatment, Chem. Eng. J., 128 (2007) 169–175.

[34] D. Elzo, I. Huisman and E. Middelink, Charge effects on inorganic membrane performance in a cross-flow microfiltration process, Colloid Surf, A., 138 (1998) 145–159.

[35] Y. Zhao, Y. Xing and N. Xu, Effects of inorganic salt on ceramic membrane microfiltration of titanium dioxide suspension, J. Membr. Sci., 254 (2005) 81–88.